



# Aviation 2006 NO<sub>x</sub>-induced effects on atmospheric ozone and HO<sub>x</sub> in Community Earth System Model (CESM)

A. Khodayari<sup>1</sup>, S. Tilmes<sup>3</sup>, S. C. Olsen<sup>2</sup>, D. B. Phoenix<sup>2</sup>, D. J. Wuebbles<sup>2</sup>, J.-F. Lamarque<sup>3</sup>, and C.-C. Chen<sup>3</sup>

<sup>1</sup>Department of Civil and Environmental Engineering, University of Illinois at Urbana-Champaign, Urbana, IL 61801, USA

<sup>2</sup>Department of Atmospheric Sciences, University of Illinois at Urbana-Champaign, Urbana, IL 61801, USA

<sup>3</sup>National Center for Atmospheric Research, Boulder, CO, USA

Received: 14 January 2014 – Accepted: 3 February 2014 – Published: 7 March 2014

Correspondence to: D. J. Wuebbles (wuebbles@illinois.edu)

Published by Copernicus Publications on behalf of the European Geosciences Union.

Title Page

Abstract

Introduction

Conclusions

References

Tables

Figures

◀

▶

◀

▶

Back

Close

Full Screen / Esc

Printer-friendly Version

Interactive Discussion



## Abstract

The interaction between atmospheric chemistry and ozone ( $O_3$ ) in the upper troposphere and lower stratosphere (UTLS) presents a major uncertainty in understanding the effects of aviation on climate. In this study, two configurations of the atmospheric model from the Community Earth System Model (CESM), CAM4 and CAM5, are used to evaluate the effects of aircraft nitrogen oxide ( $NO_x = NO + NO_2$ ) emissions on ozone and the background chemistry in the UTLS. CAM4 and CAM5 simulations were both performed with extensive tropospheric and stratospheric chemistry including 133 species and 330 photochemical reactions. CAM5 includes direct and indirect aerosol effects on clouds using a modal aerosol module (MAM) whereby CAM4 uses a bulk aerosol module which can only simulate the direct effect. To examine the accuracy of the aviation  $NO_x$  induced ozone distribution in the two models, results from the CAM5 and CAM4 simulations are compared to ozonesonde data. Aviation  $NO_x$  emissions for 2006 were obtained from the AEDT (Aviation Environmental Design Tool) global commercial aircraft emissions inventory. Differences between simulated  $O_3$  concentrations and ozonesonde measurements averaged at representative levels in the troposphere and different regions are 13 % in CAM5 and 18 % in CAM4. Results show a localized increase in aviation induced  $O_3$  concentrations at aviation cruise altitudes that stretches from 40° N to the North Pole. The results indicate a greater and more disperse production of aviation  $NO_x$ -induced ozone in CAM5, with the annual tropospheric mean  $O_3$  perturbation of 1.3 ppb (2.7 %) for CAM5 and 1.0 ppb (1.9 %) for CAM4. The annual mean  $O_3$  perturbation peaks at about 8.3 ppb (6.4 %) and 8.8 ppb (5.2 %) in CAM5 and CAM4, respectively. Aviation emissions also result in increased OH concentrations and methane ( $CH_4$ ) loss rates, reducing the tropospheric methane lifetime in CAM5 and CAM4 by 1.9 % and 1.40 %, respectively. Aviation  $NO_x$  emissions are associated with a change in global mean  $O_3$  radiative forcing (RF) of 43.9 and 36.5  $mW m^{-2}$  in CAM5 and CAM4, respectively.

ACPD

14, 6163–6202, 2014

## Aviation 2006 $NO_x$ -induced effects

A. Khodayari et al.

Title Page

Abstract

Introduction

Conclusions

References

Tables

Figures

◀

▶

◀

▶

Back

Close

Full Screen / Esc

Printer-friendly Version

Interactive Discussion



## 1 Introduction

The aviation industry has grown rapidly since its nascence, at a rate of 9 % per year for passenger traffic between 1960 and 2000 (IPCC, 1999) and is one of the fastest growing transportation sectors (IPCC, 2008). Despite several international economic and other setbacks over the last few decades, including large price increases for fuel, and a global recession, the aviation industry continues to experience growth. The 2013 FAA forecast calls for an annual average increase of 2.2 % per year in US passenger carrier growth over the next twenty years. The growth is predicted to be slightly greater for the first five years under the assumption of a faster US economic growth rate (FAA, 2013). As such, it is important to assess the potential impacts that aviation will have on future climate.

Aviation affects climate in various ways. The main concerns to climate result from the emissions of carbon dioxide (CO<sub>2</sub>) and nitrogen oxides (NO<sub>x</sub>), which influence the gas-phase and aerosol chemistry. Other aviation induced impacts result from the emissions of H<sub>2</sub>O, and the emission of sulfate and soot particles, which influence the formation of contrail-cirrus clouds and change the cloudiness by acting as cloud condensation nuclei (e.g., Gettelman et al., 2012). The resulting effects of these emissions modify the chemical properties of the upper troposphere and lower stratosphere and the cloud microphysics that affect the Earth's climate system radiative forcing. For the majority of these effects, the radiative forcing is positive; however, for sulfate particles – which reflect incoming shortwave radiation, and for the increases in OH concentrations – which reduce the CH<sub>4</sub> concentrations, the radiative forcing is negative (Lee et al., 2009). The indirect effect of aerosols on cirrus clouds may, on the other hand, result in a negative radiative forcing because of the reduction in outgoing long-wave radiation trapped by those clouds (Gettelman et al., 2012). This study will focus on the aviation NO<sub>x</sub>-induced effects, and particularly the NO<sub>x</sub>-induced effect on atmospheric ozone (O<sub>3</sub>).

There have been many previous studies that examined the effect of aviation NO<sub>x</sub> emissions on NO<sub>x</sub>-induced O<sub>3</sub> (e.g., Derwent et al., 1999, 2001; Fuglestedt et al.,

ACPD

14, 6163–6202, 2014

### Aviation 2006 NO<sub>x</sub>-induced effects

A. Khodayari et al.

Title Page

Abstract

Introduction

Conclusions

References

Tables

Figures

◀

▶

◀

▶

Back

Close

Full Screen / Esc

Printer-friendly Version

Interactive Discussion



1999; Wild et al., 2001; Stevenson and Doherty, 2004; Köhler et al., 2008; Hoor et al., 2009; Koffi et al., 2010; Hodnebrog et al., 2011). The aviation  $\text{NO}_x$ -induced changes in  $\text{O}_3$  calculated in these studies varies between 0.46 to 0.90 Dobson units of ozone per Tg N per year ( $\text{DU}(\text{O}_3) [\text{TgNyr}^{-1}]$ ). Other recent studies have examined the factors that control the production of  $\text{NO}_x$ -induced  $\text{O}_3$ . Stevenson and Derwent (2009) found that the  $\text{O}_3$  and  $\text{CH}_4$  response to  $\text{NO}_x$  emissions varies regionally, and are most sensitive in regions with low background  $\text{NO}_x$  concentrations. Several studies analyzed the impact of the location and time of the emissions (Derwent et al., 2000; Stevenson et al., 2004). Wild et al. (2012) examined the impact of solar flux variations while Shine et al. (2005) and Berntsen et al. (2005) investigated the effects of atmospheric mixing. However, as reported in Holmes et al. (2011), model-based estimates of aviation  $\text{NO}_x$ -induced changes in  $\text{O}_3$  vary by up to 100 %, largely because of differences between models in the ratios of  $\text{NO} : \text{NO}_2$  and  $\text{OH} : \text{HO}_2$ , background  $\text{NO}_x$  levels, location and time of emissions, the amount of sunlight, and in atmospheric mixing (Holmes et al., 2011). Recent studies by Olsen et al. (2013) and Brasseur et al. (2013) found considerable differences between a set of climate-chemistry models (CCMs) and chemistry transport models (CTMs) in comparisons of the background atmosphere and aviation  $\text{NO}_x$ -induced changes in ozone.

In this study, we examine the effect of aviation  $\text{NO}_x$  emissions on the atmospheric concentration of  $\text{O}_3$  and hydrogen oxide radicals ( $\text{HO}_x = \text{OH} + \text{HO}_2$ ) and the reduction of  $\text{CH}_4$  lifetime using the latest versions of the atmospheric components of the Community Earth System Model (CESM) model, namely the Community Atmosphere Model with Chemistry, Version 4 (CAM4) and Version 5 (CAM5). We further calculate the radiative forcing associated with the changes in  $\text{O}_3$  concentration using the University of Illinois Radiative Transfer Model (UIUC RTM). While the calculated effects in CAM4 and CAM5 provide a new reference for the aviation  $\text{NO}_x$ -induced effects in comprehensive climate-chemistry models, they also provide a measure for the effects that different treatments of aerosol processes can have on the aviation  $\text{NO}_x$ -induced effects. CAM4 uses a bulk aerosol module as described in Lamarque et al. (2012), while CAM5 uses

## Aviation 2006 $\text{NO}_x$ -induced effects

A. Khodayari et al.

Title Page

Abstract

Introduction

Conclusions

References

Tables

Figures

◀

▶

◀

▶

Back

Close

Full Screen / Esc

Printer-friendly Version

Interactive Discussion



a modal aerosol module (MAM) based on Liu et al. (2012). The significance of MAM is its capability of simulating aerosol size distribution and both internal and external mixing between aerosol components while treating aerosol processes and properties in a physically-based manner (Liu et al., 2012).

This paper is organized as follows. The following section provides model description. Section 3 discusses the emissions and simulation setup. Section 4 presents the results and Sect. 5 provides the concluding material.

## 2 Model description

CAM4 and CAM5 (Community Atmosphere Model versions 4 and 5) are the atmospheric component models for the Community Earth System Model (CESM) (<http://www.cesm.ucar.edu/>). The details of the physics parameterizations in the CAM4 and CAM5 models have been discussed extensively in other studies before (e.g. Neale et al., 2011; Gent et al., 2011; Lamarque et al., 2012). The released version of CAM4 and the development version of CAM5 (cesm1\_2\_beta08\_chem) were used in this study.

Both models use the same gas-phase chemical mechanisms including tropospheric and stratospheric chemistry with about 133 species and 330 photochemical reactions (Lamarque et al., 2012). A complete list of species and reactions can be found in Lamarque et al. (2012).

While the two models use the same gas-phase chemistry, there are several differences in their aerosol treatment and physics parameterization between shallow convection, planetary boundary layer (PBL) schemes, bulk microphysics, cloud macrophysics, and radiative transfer (Medeiros et al., 2012). However, a major difference between the models is that CAM4 uses a bulk aerosol module with one lognormal distribution for all aerosols (Lamarque et al., 2012) while CAM5 uses a new modal aerosol module (MAM) (Liu et al., 2012). MAM was developed with two versions, one with seven lognormal modes (MAM7) and one with three lognormal modes (MAM3)

Title Page

Abstract

Introduction

Conclusions

References

Tables

Figures

◀

▶

◀

▶

Back

Close

Full Screen / Esc

Printer-friendly Version

Interactive Discussion



Aviation 2006  
NO<sub>x</sub>-induced effects

A. Khodayari et al.

Title Page

Abstract

Introduction

Conclusions

References

Tables

Figures

I◀

▶I

◀

▶

Back

Close

Full Screen / Esc

Printer-friendly Version

Interactive Discussion



(Liu et al., 2012; Lamarque et al., 2012). Here, we use the more complete version with seven lognormal modes. MAM7 represents Aitken, accumulation, primary carbon, fine dust and sea salt, and course dust and sea salt modes. Within each mode, the mass mixing ratios of the respected aerosols and their number mixing ratios are calculated (Liu et al., 2012). MAM simulates both internal and external mixing of aerosols, chemical and optical properties of aerosols, and various complicated aerosols processes (Liu et al., 2012). Cloud microphysical processes are represented by a prognostic, two-moment formulation for cloud droplets and cloud ice. Mass and number concentrations of cloud droplets and cloud ice follow the Morrison and Gettelman (2008) parameterization. The gamma function is employed to determine liquid and ice particle sizes (Gettelman et al., 2008). The evolution of liquid and ice particles in time is affected by grid-scale advection, convective detrainment, and turbulent diffusion. Activation of cloud droplets is a function of aerosol size distribution, aerosol chemistry, temperature, and vertical velocity (Neale et al., 2011). The cloud macrophysics scheme imposes full consistency between cloud fraction and cloud condensate. Liquid cloud fraction is based on a triangular distribution of total relative humidity. Ice cloud fraction is based on Gettelman et al. (2010) that allows supersaturation via a modified relative humidity over ice and the inclusion of the ice condensate amount. The aerosols-cloud scheme simulates full aerosol-cloud interactions such as cloud droplet activation by aerosol, precipitation processes due to particle size dependence, and explicit radiative interaction of cloud particles (Liu et al., 2012).

The UIUC RTM was used offline to calculate the forcing associated with aviation NO<sub>x</sub>-induced short-term O<sub>3</sub>. Earlier versions of the UIUC RTM have been used in previous research (e.g., Jain et al., 2000; Naik et al., 2000; Youn et al., 2009; Patten et al., 2011). The UIUC RTM calculates the flux of solar and terrestrial radiation across the tropopause. The solar model includes 18 spectral bins from 0.2 to 0.5 microns and includes absorption by H<sub>2</sub>O, O<sub>3</sub>, O<sub>2</sub>, CO<sub>2</sub>, clouds, and the surface. Scattering processes by clouds, gas-phase molecules, and the surface are included as well. The terrestrial radiation calculation uses a narrow band model of absorptivity and emissivity that

covers wave numbers from 0 to 3000  $\text{cm}^{-1}$  at a resolution of 10  $\text{cm}^{-1}$  for  $\text{H}_2\text{O}$ , CFC-11, and CFC-12, and of 5  $\text{cm}^{-1}$  for all other gases. The infrared absorption parameters for gases are obtained from the HITRAN 2004 database (Rothman et al., 2005). Surface albedo and emissivity are based on observations, while clouds are based on the International Satellite Cloud Climatology Project.

### 3 Aviation $\text{NO}_x$ emissions and simulation setup

Both models were run at a horizontal resolution of  $1.9^\circ$  latitude  $\times$   $2.5^\circ$  longitude and were configured with 56 vertical levels covering from the surface up to  $\sim 2$  hPa. To reduce year-to-year climate variability in the model simulations and to help detect the aviation  $\text{NO}_x$  signal, specified dynamics (“off-line” mode) simulations were performed. In these simulations, changes in the chemical constituents do not affect the dynamics. The models used the GEOS DAS v5.1 meteorology for the year 2005 (Rienecker et al., 2008) which was the closest available assimilated meteorology data to the year of interest (2006). The aviation emissions for 2006 are from the AEDT aviation emissions analyses (Wilkerson et al., 2010; Olsen et al., 2012). The background emissions of non-aviation short-lived species (e.g.,  $\text{NO}_x$ , volatile organic compounds (VOCs)) were obtained from the IPCC RCP4.5 scenario for year 2005 (van Vuuren et al., 2011). The monthly surface concentrations of longer-lived species, e.g.,  $\text{CO}_2$ ,  $\text{CH}_4$ , chlorofluorocarbons (CFCs), and nitrous oxide ( $\text{N}_2\text{O}$ ), were specified as boundary conditions based on the IPCC RCP4.5 scenario. To analyze the effect of aviation  $\text{NO}_x$  emissions on the background atmosphere, two simulations are performed in each model. One simulation considers all  $\text{NO}_x$  emissions including aviation  $\text{NO}_x$ , and the other simulation has all  $\text{NO}_x$  emissions but no aviation  $\text{NO}_x$  (control run). The difference between these two simulations corresponds to the changes induced by aviation  $\text{NO}_x$ . The simulations were run for seven years, cycling through the 2005 meteorology, to reach steady-state with data from the 7th year used in this analysis.

Title Page

Abstract

Introduction

Conclusions

References

Tables

Figures

◀

▶

◀

▶

Back

Close

Full Screen / Esc

Printer-friendly Version

Interactive Discussion





## 4 Results and discussions

### 4.1 Chemistry diagnosis

Due to the radiative importance of ozone in the troposphere and stratosphere and in relation to differences in aerosols treatment and physics parameterization between the two models, simulated ozone in the control runs at representative altitudes is evaluated using an ozonesonde climatology (Tilmes et al., 2012). This climatology includes observations for the years 1995–2011 and covers averaged ozone profiles for 41 different ozonesonde stations that are grouped into 12 regions. For our comparisons, we evaluate ozone at four pressure levels covering the troposphere and lower stratosphere (50, 250, 500, and 900 hPa) over the 12 areas, which are grouped into three larger regions (Tropics, Mid-Latitudes, and High Latitudes), as shown in Fig. 1. Model results are interpolated horizontally to all the stations within each region, and averaged over each region. The comparison between model and observations is illustrated in Taylor-like diagrams for each of the corresponding pressure levels and regions. A slightly different version of CAM4 including chemistry has been previously tested against ozone observations as well as the observations of other major atmospheric compounds (e.g., Lamarque et al., 2012).

The two model versions are in good agreement at 50 hPa, but for most locations, the models overestimate the observed ozone concentration. However, CAM5 underestimates ozone at the NH Poles, Canada, and Western Europe. CAM4 and CAM5 perform best in NH High Latitudes and Mid-Latitudes regions (with the exception of Japan). The average absolute percent difference in simulated ozone for all locations is 13.8 % in CAM5 and 14.4 % in CAM4. With the exception of the W-Pacific/E-Indian Ocean in CAM4 and the Atlantic/Africa region in CAM5, both models resolve the seasonal correlation quite well at 50 hPa. The average seasonal correlation is 0.83 in CAM5 and 0.84 in CAM4. Overall, both models are similar in their representations of ozone at 50 hPa.

At 250 hPa, CAM5 performs better than CAM4 with a smaller percent difference between simulated ozone and observations. At all locations, CAM4 simulates higher

Title Page

Abstract

Introduction

Conclusions

References

Tables

Figures

◀

▶

◀

▶

Back

Close

Full Screen / Esc

Printer-friendly Version

Interactive Discussion





## Aviation 2006 NO<sub>x</sub>-induced effects

A. Khodayari et al.

Title Page

Abstract

Introduction

Conclusions

References

Tables

Figures

◀

▶

◀

▶

Back

Close

Full Screen / Esc

Printer-friendly Version

Interactive Discussion



ozone concentrations than CAM5. For NH High Latitudes, both models greatly underestimate ozone (18–26 %). In the mid-latitudes and tropics, both models overestimate ozone. The overestimate of ozone in the mid-latitudes and tropics in CAM4 was also found in Lamarque et al. (2012), who noted that this result is an indication of a model estimated tropopause that is lower than observed. The seasonal cycle agrees well with observations for the mid- and high latitude locations. The average correlation coefficient of monthly averages between the models and observations is 0.75, indicating a good representation of the seasonal ozone cycle.

Of the four pressure levels studied, the models most accurately simulate ozone at the 500 hPa level. The absolute difference in generated ozone is within 11.7 % for both models, which is within the variability of the observations. CAM5 underestimates ozone at nine of the twelve locations evaluated at this pressure level. CAM4, on the other hand, overestimates ozone at all but one location. Overall, CAM5 appears to perform better than CAM4 due to a lower percent difference in ozone (6.0 % in CAM5 compared to 11.7 % in CAM4). The seasonal cycle is simulated reasonably well for both models, with a correlation coefficient of 0.80 for CAM5 and 0.82 for CAM4.

On average, both models perform well in the lowest level (900 hPa), although there are several outliers. Both models overestimate the ozone concentration in the Western Europe and Canada regions. On the other hand, both models underestimate ozone in the SH Mid-Latitude and SH Polar regions. At all other locations, however, the estimated ozone is very accurate. The relative bias is lower in CAM5 (10.0 % compared to 15.7 % in CAM4), indicating a better representation of ozone by CAM5. Additionally, with the exception of the Equatorial Americas region in CAM4 and the Japan region for both models, the seasonal correlation is excellent (0.81 in both CAM5 and CAM4).

Overall, both models represent ozone well (on average to within 13 % in CAM5 and 18 % in CAM4 for all the locations) in the troposphere and stratosphere. The seasonal cycle is also very accurate in the models. In general, CAM4 tends to overestimate ozone, more so than CAM5, which occasionally underestimates ozone – especially at

lower levels. CAM5, however, appears to be slightly more accurate at estimating ozone than CAM4.

Model diagnostic tests were also done for  $\text{HNO}_3$ ,  $\text{NO}$ ,  $\text{NO}_2$ ,  $\text{NO}_x$ , and  $\text{OH}$ , using the chemistry diagnostics package available at <http://www.cgd.ucar.edu/amp/amwg/diagnostics/>. The diagnostics package was used to compare the CAM4 and CAM5 simulations with observational data, collected from aircraft measurements from several campaigns. Overall, in the mid-troposphere (4–8 km) where the majority of the observations were taken, both CAM4 and CAM5 simulated concentrations and distributions of these gases are within the central 50 % and 90 % of the available observations; and both models are in good agreement with each other and the results found in Lamarque et al. (2012). The additional diagnoses and the related discussion are provided in Supplement.

## 4.2 Spatial distribution of $\text{NO}_x$ emissions

The AEDT  $\text{NO}_x$  emission data used as the input to the model runs had an hourly temporal resolution. The spatial distribution of aviation  $\text{NO}_x$  emissions for 2006 is shown in Fig. 2 which amounts to  $2.7 \text{ Tg } (\text{NO}_2) \text{ yr}^{-1}$ . As in Fig. 2, the largest intensity of  $\text{NO}_x$  emissions is in the eastern United States, eastern Asia, and Europe. The local maximum in the eastern US contributes approximately  $0.0136 \text{ Tg}$  to the global emissions of  $\text{NO}_2$  while the local maximum in Europe contributes  $0.0154 \text{ Tg}$ . Additionally, the peak value in Asia contributes  $0.0123 \text{ Tg}$  to the global total. These values represent the maximum emissions from a single grid cell. The main source of  $\text{NO}_x$  emissions occur between  $30^\circ$  and  $60^\circ \text{ N}$  latitude.

Figure 3 shows the seasonal distribution of aviation  $\text{NO}_x$  emissions from 2006. As shown in Fig. 3, aviation  $\text{NO}_x$  emissions have a different seasonal distribution with the highest amount of emissions released in the summer, due to increased air traffic in those months.

Title Page

Abstract

Introduction

Conclusions

References

Tables

Figures

◀

▶

◀

▶

Back

Close

Full Screen / Esc

Printer-friendly Version

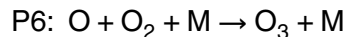
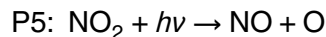
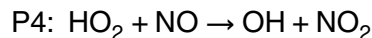
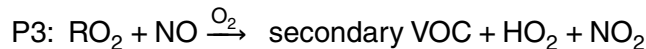
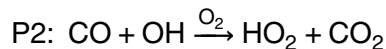
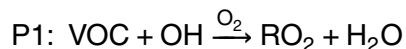
Interactive Discussion



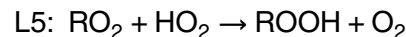
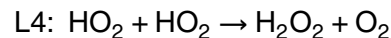
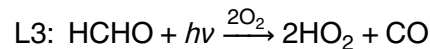
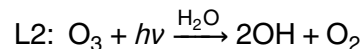
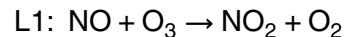
### 4.3 Ozone

Figure 4 shows the aviation  $\text{NO}_x$ -induced annual vertical profile of  $\text{O}_3$  production and loss as calculated by CAM5 (red) and CAM4 (blue). Both models show the maximum rate of ozone production peaking in the upper troposphere/lower stratosphere (UTLS) region where the greatest amount of aircraft induced  $\text{NO}_x$  emissions occur.

As we analyze the results from the model runs, we use the following chemical reactions for ozone production in the troposphere (Sillman, 2012):



Ozone destruction in the troposphere, on the other hand, is given by the following reactions (Sillman, 2012):





The impact of aviation induced  $\text{NO}_x$  on ozone results in a net increase in ozone with a maximum around 250 hPa, and a net decrease in ozone below 450 hPa. Within the UTLS region, the rate of ozone loss decreases due to the increase in  $\text{HO}_2$  (Fig. 8, as discussed below) reacting with NO (as in Eq. P4). This process creates  $\text{NO}_2$  which further increases  $\text{O}_3$  production (by Eqs. P5 and P6). Part of the excess ozone that is created in the UTLS region is transported to lower altitudes. As shown in Fig. 4, the rate of ozone loss peaks around 500 hPa. As described by Eq. (L2), at this altitude, excess ozone transported from the UTLS region in the presence of water vapor reacts to form  $\text{HO}_x$ , increasing ozone loss. Additional reductions in the net  $\text{O}_3$  production are caused by the increased reaction of  $\text{HO}_x$  with  $\text{NO}_x$  near the surface, resulting in the conversion of  $\text{NO}_x$  to  $\text{HNO}_3$  (Eq. L6).

While the patterns of the changes in the simulated ozone production and loss agree well between the models and with previous studies (Köhler et al., 2008), there are differences between CAM4 and CAM5 in the magnitudes. Compared to CAM4, overall ozone production and loss are larger in CAM5, due to the differences in OH between the models. The net rate of ozone production in CAM5 is higher at cruise altitudes and slightly lower at lower altitudes. The maximum net production of ozone is  $1.2 \times 10^{20} \text{ molecules s}^{-1} \text{ Pa}^{-1}$  in CAM5 and  $1.0 \times 10^{20} \text{ molecules s}^{-1} \text{ Pa}^{-1}$  in CAM4. CAM4 estimates a maximum rate of production at  $1.2 \times 10^{20} \text{ molecules s}^{-1} \text{ Pa}^{-1}$  while CAM5 estimates a rate of  $1.5 \times 10^{20} \text{ molecules s}^{-1} \text{ Pa}^{-1}$ . At lower altitudes, CAM5 gives a greater rate of ozone loss than CAM4. Both models show a peak in the ozone loss rate around 600 hPa with values of about  $0.6 \times 10^{20} \text{ molecules s}^{-1} \text{ Pa}^{-1}$  in CAM5, and about  $0.4 \times 10^{20} \text{ molecules s}^{-1} \text{ Pa}^{-1}$  in CAM4. Overall, as found in Fig. 1 (as confirmed through comparisons with ozonesonde data) and shown in Fig. 4, CAM5 is more efficient in producing ozone than CAM4 in most of the atmosphere.

Title Page

Abstract

Introduction

Conclusions

References

Tables

Figures

◀

▶

◀

▶

Back

Close

Full Screen / Esc

Printer-friendly Version

Interactive Discussion



## 4.4 Global burdens

Table 1 compares the annual mean tropospheric burden of  $\text{HO}_x$ ,  $\text{NO}_x$ ,  $\text{NO}_y$  and the ratios of  $\text{OH} : \text{HO}_2$  and  $\text{NO}_x : \text{NO}_y$  in both CAM4 and CAM5 for both the control run and aviation  $\text{NO}_x$ -perturbed run. The comparison of the burdens presented in Table 1 indicates that the background atmosphere is relatively different between the two models (e.g.  $\sim 14\%$  difference in the background  $\text{O}_3$ ) While such differences seem to be small compared to the intermodal uncertainty ( $\pm 25\%$ ) reported in Stevenson et al. (2006), there is about a 12.5% difference in the aviation  $\text{NO}_x$ -induced annual mean tropospheric  $\text{O}_3$  response.

To explore the cause of higher aviation  $\text{NO}_x$ -induced  $\text{O}_3$  production in CAM5, we compare the burden of  $\text{HO}_x$ ,  $\text{NO}_x$  and  $\text{NO}_y$  (all the nitrogen containing compounds in the gas phase) at cruise region in both CAM4 and CAM5. Table 2 shows the annual burden of  $\text{HO}_x$ ,  $\text{NO}_x$ ,  $\text{NO}_y$  and the ratios of  $\text{OH} : \text{HO}_2$  and  $\text{NO}_x : \text{NO}_y$  between 200–400 hPa and between 30–60° N in both CAM4 and CAM5 for both the control and aviation  $\text{NO}_x$ -perturbed run. As shown in Table 2, the ratio of  $\text{OH} : \text{HO}_2$  is about 24% higher in the CAM5 perturbed run than in the CAM4 perturbed run. This excess OH in CAM5 results in higher ozone production by the initial reaction of the ozone production sequence (P1) and implies higher NO to  $\text{NO}_2$  conversion (P4). The ratio of  $\text{NO}_x : \text{NO}_y$  is approximately the same between the models; however, the  $\text{NO}_y$  burden is about 16% higher in the CAM5 perturbed run than in the CAM4 perturbed run. This indicates lower conversion of  $\text{NO}_y$  to the aerosol phase and more  $\text{NO}_x$  available in the CAM5 perturbed run to trigger the ozone formation reactions, resulting in higher ozone production. A more detailed analysis of the magnitude and the pattern of aviation  $\text{NO}_x$ -induced changes in ozone and  $\text{HO}_x$  are discussed below.

The aviation  $\text{NO}_x$ -induced ozone perturbation is shown in Fig. 5. Model results from CAM5 are shown on the top panel while CAM4 is on the bottom. The left column shows the mean zonal ozone perturbation for January, while the right column shows July. As shown in Fig. 5, CAM5 produces a greater amount and wider distribution of

Title Page

Abstract

Introduction

Conclusions

References

Tables

Figures

◀

▶

◀

▶

Back

Close

Full Screen / Esc

Printer-friendly Version

Interactive Discussion



Aviation 2006  
NO<sub>x</sub>-induced effects

A. Khodayari et al.

Title Page

Abstract

Introduction

Conclusions

References

Tables

Figures

I◀

▶I

◀

▶

Back

Close

Full Screen / Esc

Printer-friendly Version

Interactive Discussion



ozone in the UTLS region for both months. The pattern and the localized maximum of the ozone perturbation at 200 hPa in the NH are about the same in both CAM4 and CAM5. The tropospheric mean change in O<sub>3</sub> is higher in CAM5 than CAM4 for both January and July. In July, CAM5 generates a tropospheric mean ozone perturbation of 1.2 ppb (compared to 1.0 in CAM4). In January, CAM5 generates a tropospheric mean ozone perturbation of 1.3 ppb (compared to 1.1 in CAM4). Overall, aviation NO<sub>x</sub> emissions from the year 2006 yield an annual tropospheric mean O<sub>3</sub> perturbation of 1.3 ppb (2.7 %) in CAM5 and 1.0 ppb (1.9 %) in CAM4. The annual mean O<sub>3</sub> perturbation peaks at 8.3 ppb (6.4 %) in CAM5 and 8.8 ppb (5.2 %) in CAM4. Despite the greater production of annual mean O<sub>3</sub> in CAM5, the peak is slightly lower in CAM5 compared to CAM4, since the produced O<sub>3</sub> is more distributed towards the surface in CAM5.

As shown in Fig. 5, the UTLS ozone perturbation is much greater in July than in January for both models. This is due to differences in the length of daylight between those months, increased photochemistry, and higher aviation NO<sub>x</sub> emissions in July (as shown in Fig. 3). The increased daylight allows more photolysis of NO<sub>2</sub> to occur, which generates O<sub>3</sub> (Eqs. P5 and P6). Also note the differences in ozone perturbations in the lower troposphere between January and July. In the summer, the ozone perturbation at lower altitudes is weaker due to greater surface deposition and also the shorter photochemical lifetime of ozone through increased water vapor (and more HO<sub>x</sub> giving increased ozone loss) (Hodnebrog et al., 2011). Additionally, both models show the maximum ozone impact increasing towards high latitudes in the NH in July. A similar result was found by Hoor et al. (2009) who showed a maximum zonal mean ozone perturbation centered around 75° N during June.

As shown in both months and models, a mid-latitudinal perturbation extends from 400 hPa down towards the surface. This feature agrees with past studies by Hoor et al. (2009), Koffi et al. (2010), and Hodnebrog et al. (2011). Hoor et al. (2009) notes that this feature is due to more vigorous boundary layer mixing and convective transport into the free troposphere during the summer.

Aviation 2006  
NO<sub>x</sub>-induced effects

A. Khodayari et al.

Title Page

Abstract

Introduction

Conclusions

References

Tables

Figures

◀

▶

◀

▶

Back

Close

Full Screen / Esc

Printer-friendly Version

Interactive Discussion



As shown in Fig. 6, annual mean column ozone changes are relatively zonally well mixed, however, several “hotspots” in both CAM5 and CAM4 exist just north of the Mediterranean and off the western coast of Europe. A more uniform spread is seen over Europe, the western half of Asia, the Atlantic Ocean and a small strip at about 45° N in the Pacific Ocean. These “hotspots” are stronger in CAM5 and peak at about 2.3 DU compared to 2.1 DU in CAM4. As expected, the ozone impact is very small in the SH. A sharp ozone gradient exists in the NH subtropics, as was also seen in previous studies. The ozone concentration continues to increase, with the maximum values between 30 and 60° N. Hoor et al. (2009) and Hodnebrog et al. (2011) found a similar distribution. Overall, aviation NO<sub>x</sub> emissions from the year 2006 lead to a 1.0 and 0.9 DU change in annual global mean ozone column in CAM5 and CAM4, respectively.

#### 4.4.1 HO<sub>x</sub>

The hydroxyl radical (OH) plays an important role in the creation of atmospheric ozone. It is the primary oxidizing agent of the troposphere, removing greenhouse gases such as CH<sub>4</sub>, CO, HCFCs, and others. Production of OH by O<sub>3</sub> is given by Eq. (L2). Figure 7 shows the aviation induced zonal mean annual OH perturbations.

Similar to ozone, the impact of aviation emitted NO<sub>x</sub> on tropospheric OH production is largest in July. This increase in OH during the summer months is also due to the enhanced photochemistry. Aircraft emissions have the largest zonal mean ozone impact in the UTLS region in mid- and high latitudes in the NH between 40–90° N. However, the OH perturbation is more concentrated south of the O<sub>3</sub> perturbations. The more southern position of OH is due to the increased humidity and the lower solar zenith angle, which are essential to produce the excited oxygen atom (O(<sup>1</sup>D)) and hence higher OH concentrations. This result agrees well with recent studies by Hoor et al. (2009) and Hodnebrog et al. (2011). Additionally, there is a greater perturbation of OH extending towards the surface over mid-latitudes than there was of O<sub>3</sub>. This is due to the increased production of HO<sub>x</sub> in the mid-troposphere triggered by O<sub>3</sub> photolysis. Additionally, both models show OH perturbations extending from 400 hPa down to the surface above



40° N. This feature is much weaker in January because the UV actinic flux necessary for OH production is much smaller in the NH. Between the two models, the OH concentration is higher in CAM5 than CAM4. This is a result of higher O<sub>3</sub> production in CAM5. In July, the CAM5 aviation NO<sub>x</sub>-induced tropospheric mean OH perturbation is  $1.4 \times 10^4$  molecules cm<sup>-3</sup> (compared to  $9.1 \times 10^3$  in CAM4). In January, the CAM5 aviation NO<sub>x</sub>-induced tropospheric mean OH perturbation is  $9.7 \times 10^3$  molecules cm<sup>-3</sup> (compared to  $6.4 \times 10^3$  in CAM4). Overall, aviation NO<sub>x</sub> emissions from the year 2006 lead to an annual tropospheric mean OH perturbation of  $1.2 \times 10^4$  molecules cm<sup>-3</sup> in CAM5 and  $7.8 \times 10^3$  molecules cm<sup>-3</sup> in CAM4.

Figure 8 shows the CAM4 and CAM5 HO<sub>2</sub> perturbations due to aviation NO<sub>x</sub> emissions. Areas that experience an increase in HO<sub>2</sub> concentrations are shown in red and areas that experience a decrease in HO<sub>2</sub> are in blue. Increases in NO<sub>x</sub> emissions from aviation increases OH levels by shifting the HO<sub>x</sub> balance in favor of OH production, given by equation P4 (Stevenson et al., 2004; Berntsen et al., 2005; Köhler et al., 2008). This process results in HO<sub>2</sub> loss at cruise altitudes. As expected, the areas of HO<sub>2</sub> loss correspond to the areas that experienced an increase in OH concentrations.

In January, there is a greater rate of HO<sub>2</sub> consumption in the UTLS region in CAM5 than there is in CAM4 due to higher OH production. Following Eq. (P4), this HO<sub>2</sub> reacts with aircraft emitted NO to give OH and NO<sub>2</sub>. Similarly, the rate of HO<sub>2</sub> consumption is also greater in the UTLS region during July in CAM5 as well. When comparing Fig. 8 with Fig. 7, the locations of maximum HO<sub>2</sub> loss correspond with the locations of maximum OH concentrations, indicating that reaction (P4) is a significant reaction in OH production in the UTLS region. At lower altitudes in July, the transported ozone is photolyzed in the presence of water vapor, thus increasing HO<sub>x</sub>.

## Aviation 2006 NO<sub>x</sub>-induced effects

A. Khodayari et al.

Title Page

Abstract

Introduction

Conclusions

References

Tables

Figures

◀

▶

◀

▶

Back

Close

Full Screen / Esc

Printer-friendly Version

Interactive Discussion



#### 4.4.2 CH<sub>4</sub>

The hydroxyl radical OH is the largest sink of CH<sub>4</sub> in the atmosphere. As the OH concentration is effected by aircraft emissions, so is the methane concentration and its lifetime.

Figure 9 shows the aviation induced annual zonal averaged CH<sub>4</sub> loss rate for CAM5 (left) and CAM4 (right). In both CAM5 and CAM4, the methane loss is mostly confined to the NH at a location south of the OH perturbation (between 0–30° N). This predominately occurs due to the increase in the methane-OH reaction rate constant with higher temperatures at lower altitudes. As such, in both models the position of the maximum CH<sub>4</sub> loss is below the cruise altitude. As shown in Fig. 9, the CH<sub>4</sub> loss is higher in CAM5 than CAM4 due to the higher production of aviation induced OH in CAM5. Table 3 shows the reduction in methane lifetimes as calculated for both CAM4 and CAM5.

Table 3 shows the global annual average CH<sub>4</sub> lifetimes against reaction with OH, as calculated by CAM4 and CAM5 for the background (control) run and the NO<sub>x</sub>-perturbed run. The change in CH<sub>4</sub> lifetime is also presented as the percent change in lifetime. The reduction in CH<sub>4</sub> lifetime calculated in CAM5 and CAM4 is 1.90 % (2.32 % [TgNyr<sup>-1</sup>]<sup>-1</sup>) and 1.40 % (1.71 % [TgNyr<sup>-1</sup>]<sup>-1</sup>), respectively, excluding the feedback of changes in methane concentration on its own lifetime. The CAM4 reduction in CH<sub>4</sub> lifetime falls within the  $-1.4 \pm 0.4$  % [TgNyr<sup>-1</sup>]<sup>-1</sup> to  $-1.6 \pm 0.37$  % [TgNyr<sup>-1</sup>]<sup>-1</sup> range reported by Hodnebrog et al. (2011). The CAM5 simulated change in CH<sub>4</sub> lifetime is greater than the upper range reported by Hodnebrog et al. (2011). Inclusion of the aviation induced methane feedback on its lifetime further decreases the lifetime by a factor of 1.4. The greater reduction of the CH<sub>4</sub> lifetime in CAM5 is the result of a greater increase in the aviation induced OH concentration in CAM5.

Title Page

Abstract

Introduction

Conclusions

References

Tables

Figures

◀

▶

◀

▶

Back

Close

Full Screen / Esc

Printer-friendly Version

Interactive Discussion



## 4.5 Aviation NO<sub>x</sub>-induced ozone radiative forcings

The aviation NO<sub>x</sub>-induced O<sub>3</sub> RFs were calculated as the difference of the radiation imbalance between the NO<sub>x</sub>-perturbed and control simulations at the tropopause calculated with the UIUC RTM, excluding the effects of stratospheric adjustment. Figure 10 shows the yearly averaged short-term ozone RF for CAM5 (left) and CAM4 (right). Both models show the greatest RF in the NH between 30–60° N. As expected, the O<sub>3</sub> RF from aviation is low in the SH. The greatest RF values in the SH are over the SH tropical Pacific Ocean and are most likely due to air traffic between Australia and the United States. Interestingly, radiative forcing values over Asia are relatively low, given the amount of NO<sub>x</sub> emissions from this area. Additionally, it appears that the maximum radiative forcing from Europe's emissions has shifted to the Mediterranean, indicating that these aircraft emissions have a maximum impact downwind of the source. These results agree well with Hodnebrog et al. (2011).

The associated global mean ozone RF is 43.9 and 36.5 mW m<sup>-2</sup> in CAM5 and CAM4, respectively. CAM5 has a greater annual ozone RF, due to the greater ozone perturbation, which largely accounts for the differences in radiative forcings. Only the effects of short-term ozone were considered for this study.

## 5 Conclusion

CAM5 and CAM4 simulate background ozone to within 13 % and 18 % (on average and at all the locations), respectively, compared to ozonesonde datasets. Based on the comparison with ozonesonde observations, CAM5 was more accurate at determining the ozone distribution in the troposphere and lower stratosphere. Additionally, CAM4 and CAM5 simulated concentrations of HNO<sub>3</sub>, NO, NO<sub>2</sub>, NO<sub>x</sub>, and OH are in good agreement with observations (within the central 50 % and 90 % of the available observations). CAM5 is more accurate than CAM4 for all these gases except for OH.

Title Page

Abstract

Introduction

Conclusions

References

Tables

Figures

◀

▶

◀

▶

Back

Close

Full Screen / Esc

Printer-friendly Version

Interactive Discussion



## Aviation 2006 NO<sub>x</sub>-induced effects

A. Khodayari et al.

Title Page

Abstract

Introduction

Conclusions

References

Tables

Figures

◀

▶

◀

▶

Back

Close

Full Screen / Esc

Printer-friendly Version

Interactive Discussion



Aviation induced O<sub>3</sub> is higher in CAM5 than CAM4; the annual tropospheric mean O<sub>3</sub> perturbation is 1.3 ppb (2.7 %) in CAM5 and 1.0 ppb (1.9 %) in CAM4. In July CAM5 generates an aviation NO<sub>x</sub>-induced tropospheric mean ozone perturbation of 1.2 ppb (compared to 1.0 in CAM4) with a corresponding value of 1.3 ppb in January (compared to 1.1 in CAM4).

As found in previous studies, the maximum effect from aircraft NO<sub>x</sub> emissions on ozone is in the NH Upper Troposphere/Lower Stratosphere region. This is due to the high frequency of subsonic aircraft flying in this region. The aircraft-induced ozone perturbation is greater in the NH summer due to the enhanced photochemistry. In January, the ozone perturbation mixes more towards the surface due to the shorter photochemical lifetime of ozone and the slower surface deposition rate than in July.

The hydroxyl perturbations are located to the south and at a lower altitude than the position of the maximum change in ozone. This is due to the lower zenith angle and increased humidity which are essential to produce the excited oxygen atom (O(<sup>1</sup>D)) and hence higher OH concentrations. Overall, the aviation NO<sub>x</sub>-induced change in OH is higher in CAM5 in accordance with higher ozone production. The induced changes in OH concentrations increase the methane (CH<sub>4</sub>) loss rate and reduce its lifetime by 1.90 % and 1.40 % in CAM5 and CAM4, respectively.

Results indicate a global mean O<sub>3</sub> RF of 43.9 and 36.5 mW m<sup>-2</sup> in CAM5 and CAM4, respectively. Both models agree that the maximum O<sub>3</sub> radiative forcing is between 30–60° N. However, it is interesting to note that it appears that the maximum RF is downwind of a local maximum NO<sub>x</sub> source.

This study is the first evaluation of aviation NO<sub>x</sub> effects in CAM5 which simulates the size distribution of aerosols, both internal and external mixing of aerosols, chemical and optical properties of aerosols and various complicated aerosols processes. It is noted that while the simulated change in ozone is relatively different between the two models, it is considerably smaller than the current estimates of the uncertainty in aviation effects on ozone. More detailed analyses are required to explore the impact of the differences

in the representation of the background atmosphere on aviation NO<sub>x</sub>-induced effects to a greater extent.

**Supplementary material related to this article is available online at**  
**[http://www.atmos-chem-phys-discuss.net/14/6163/2014/](http://www.atmos-chem-phys-discuss.net/14/6163/2014/acpd-14-6163-2014-supplement.pdf)**  
**[acpd-14-6163-2014-supplement.pdf](http://www.atmos-chem-phys-discuss.net/14/6163/2014/acpd-14-6163-2014-supplement.pdf).**

*Acknowledgements.* The authors would like to thank the Federal Aviation Administration, Aviation Climate Change Research Initiative (ACCRI) for support under Contract #: 10-C-NE-UI amendment 001 and The Partnership for Air Transportation Noise and Emissions Reduction (PARTNER). The opinions, findings, and conclusions or recommendations expressed in this material are those of the authors and do not necessarily reflect the views of ACCRI, PARTNER, or the FAA. This work was partially supported by the US Department of Transportation, the Illinois Department of Transportation and the Transportation Research and Analysis Computing Center. The authors would like to thank the National Center for Atmospheric Research (NCAR) for the support with computing time and NCAR is supported by the National Science Foundation (NSF). The CESM project (which includes CAM4, CAM5 and CAM-chem) is supported by the National Science Foundation and the Office of Science (BER) of the US Department of Energy. The authors would like to also thank Francis Vitt (NCAR) for his help in integrating aviation NO<sub>x</sub> emissions into CAM5.

## References

- Arnold, F., Scheid, J., Stilp, T., Schlager, H., and Reinhardt, M. E.: Measurements of jet aircraft emissions at cruise altitude I: the odd-nitrogen gases NO, NO<sub>2</sub>, HNO<sub>2</sub> and HNO<sub>3</sub>, *Geophys. Res. Lett.*, 19, 2421–2424, 1992.
- Beck, J. P., Reeves, C. E., De Leeuw, F. A., and Penkett, S. A.: The effect of aircraft emissions on tropospheric ozone in the Northern Hemisphere, *Atmos. Environ.*, 26, 17–29, 1992.
- Berntsen, T. K., Fuglestad, J. S., Joshi, M. M., Shine, K. P., Stuber, N., Ponater, M., Sausen, R., Hauglustaine, D. A., and Li, L.: Response of climate to regional emissions of ozone precursors: sensitivities and warming potentials, *Tellus B*, 57, 283–304, 2005.

Title Page

Abstract

Introduction

Conclusions

References

Tables

Figures

◀

▶

◀

▶

Back

Close

Full Screen / Esc

Printer-friendly Version

Interactive Discussion



- Borucki, W. J., Whitten, R. C., Watson, V. R., Woodward, H. T., Riegel, C. A., Capone, L. A., and Becker, T.: Model predictions of latitude-dependent ozone depletion due to supersonic transport operations, *AIAA J.*, 14, 1738–1745, 1976.
- Brasseur, G. P., Müller, J.-F., and Granier, C.: Atmospheric impact of NO<sub>x</sub> emissions by subsonic aircraft: a three-dimensional model study, *J. Geophys. Res.*, 101, 1423–1428, 1996.
- Brasseur, P. G., Weber, B., Damoah, R., Douglass, A. R., Jacobson, M. Z., Lee, H., Liang, Q., Olsen, S. C., Oman, L. D., Ott, L., Pawson, S., Selkirk, H., Sokolov, A., Stolarski, R. S., Unger, N., and Wuebbles, D. J.: Model intercomparison of ozone sensitivity to NO<sub>x</sub> emissions in the vicinity of the extratropical tropopause, *Geophys. Res. Lett.*, submitted, 2013.
- Climatic Impact Assessment Program (CIAP): Report of Findings, The Effects of Stratospheric Pollution by Aircraft, Rep. DOT-TST-75-50, US Dep. of Transp., Washington, DC, 1974.
- Collins, W. J., Bellouin, N., Doutriaux-Boucher, M., Gedney, N., Halloran, P., Hinton, T., Hughes, J., Jones, C. D., Joshi, M., Liddicoat, S., Martin, G., O'Connor, F., Rae, J., Senior, C., Sitch, S., Totterdell, I., Wiltshire, A., and Woodward, S.: Development and evaluation of an Earth-System model – HadGEM2, *Geosci. Model Dev.*, 4, 1051–1075, doi:10.5194/gmd-4-1051-2011, 2011.
- Crutzen, P. J.: SST's: a threat to the Earth's ozone shield, *Ambio*, 1, 41–51, 1972.
- Dameris, M., Grewe, V., Köhler, I., Sausen, R., Bruhl, C., Grooss, J. U., and Steil, B.: Impact of aircraft NO<sub>x</sub> emissions on tropospheric and stratospheric ozone, Part II: 3-D model results, *Atmos. Environ.*, 32, 3185–3199, 1998.
- Derwent, R. G.: Two-dimensional model studies of the impact of aircraft exhaust emissions on tropospheric ozone, *Atmos. Environ.*, 18, 1997–2007, 1982.
- Derwent, R. G., Collins, W. J., Johnson, C. E., and Stevenson, D. S.: Transient behavior of tropospheric ozone precursors in a global 3-D CTM and their indirect greenhouse effects, *Climatic Change*, 49, 463–487, 2001.
- Emmons, L. K., Walters, S., Hess, P. G., Lamarque, J.-F., Pfister, G. G., Fillmore, D., Granier, C., Guenther, A., Kinnison, D., Laepple, T., Orlando, J., Tie, X., Tyndall, G., Wiedinmyer, C., Baughcum, S. L., and Kloster, S.: Description and evaluation of the Model for Ozone and Related chemical Tracers, version 4 (MOZART-4), *Geosci. Model Dev.*, 3, 43–67, doi:10.5194/gmd-3-43-2010, 2010.
- Fitcher, C., Marquart, S., Sausen, R., and Lee, D. S.: The impact of cruise altitude on contrails and related radiative forcing, *Meteorol. Z.*, 14, 563–572, 2005.

Title Page

Abstract

Introduction

Conclusions

References

Tables

Figures

◀

▶

◀

▶

Back

Close

Full Screen / Esc

Printer-friendly Version

Interactive Discussion



- Flatøy, F. and Hov, Ø.: Three-dimensional model studies of the effect of NO<sub>x</sub> emissions from aircraft on ozone in the upper troposphere over Europe and the North Atlantic, *J. Geophys. Res.*, 101, 1401–1422, 1996.
- Fuglestad, J. S., Berntsen, T., Isaksen, I. S. A., Huiting, M., Liang, X.-Z., and Wang, W.-C.: Climatic forcing of nitrogen oxides through changes in tropospheric ozone and methane; global 3-D model studies, *Atmos. Environ.*, 33, 961–977, 1999.
- Gauss, M., Myhre, G., Pitari, G., Prather, M. J., Isaksen, I. S. A., Berntsen, T. K., Brasseur, G. P., Dentener, F. J., Derwent, R. G., Hauglustaine, D. A., Horowitz, L. W., Jacob, D. J., Johnson, M., Law, K. S., Mickley, L. J., Müller, J.-F., Plantévin, P.-H., Pyle, J. A., Rogers, H. L., Stevenson, D. S., Sundet, J. K., van Weele, M., and Wild, O.: Radiative forcing in the 21st century due to ozone changes in the troposphere and the lower stratosphere, *J. Geophys. Res.-Atmos.*, 108, 4292, doi:10.1029/2002JD002624, 2003.
- Gauss, M., Isaksen, I. S. A., Lee, D. S., and Søvde, O. A.: Impact of aircraft NO<sub>x</sub> emissions on the atmosphere – tradeoffs to reduce the impact, *Atmos. Chem. Phys.*, 6, 1529–1548, doi:10.5194/acp-6-1529-2006, 2006.
- Gent, P. R., Danabasoglu, G., Donner, L. J., Holland, M. M., Hunke, E. C., Jayne, S. R., Lawrence, D. M., Neale, R. B., Rasch, P. J., Vertenstein, M., Worley, P. H., Yang, Z.-L., and Zhang, M.: The community climate system model version 4, *J. Climate*, 24, 4973–4991, 2001.
- Gettelman, A., Morrison, H., and Ghan, S. J.: A new two-moment bulk stratiform cloud microphysics scheme in the NCAR Community Atmosphere Model (CAM3), Part II: Single-column and global results, *J. Climate*, 21, 3660–3679, 2008.
- Gettelman, A., Liu, X., Ghan, S. J., Morrison, H., Park, S., Conley, A. J., Klein, S. A., Boyle, J., Mitchell, D. L., and Li, J.-L. F.: Global simulations of ice nucleation and ice supersaturation with an improved cloud scheme in the Community Atmosphere Model, *J. Geophys. Res.*, 115, D18216, doi:10.1029/2009JD013797, 2010.
- Gettelman, A., Liu, X., Barahona, D., Lohmann, U., and Chen, C.: Climate impacts of ice nucleation, *J. Geophys. Res.*, 117, D20201, doi:10.1029/2012JD017950, 2012.
- Hesstvedt, E.: Reduction of stratospheric ozone from high-flying aircraft, studied in a two-dimensional photochemical model with transport, *Can. J. Chemistry*, 52, 1592–1598, 1974.
- Hodnebrog, Ø., Berntsen, T. K., Dessens, O., Gauss, M., Grewe, V., Isaksen, I. S. A., Koffi, B., Myhre, G., Olivé, D., Prather, M. J., Pyle, J. A., Stordal, F., Szopa, S., Tang, Q., van Velthoven, P., Williams, J. E., and Ødemark, K.: Future impact of non-land based traffic

## Aviation 2006 NO<sub>x</sub>-induced effects

A. Khodayari et al.

Title Page

Abstract

Introduction

Conclusions

References

Tables

Figures

◀

▶

◀

▶

Back

Close

Full Screen / Esc

Printer-friendly Version

Interactive Discussion





Aviation 2006  
NO<sub>x</sub>-induced effects

A. Khodayari et al.

Title Page

Abstract

Introduction

Conclusions

References

Tables

Figures

◀

▶

◀

▶

Back

Close

Full Screen / Esc

Printer-friendly Version

Interactive Discussion



emissions on atmospheric ozone and OH – an optimistic scenario and a possible mitigation strategy, *Atmos. Chem. Phys.*, 11, 11293–11317, doi:10.5194/acp-11-11293-2011, 2011.

Holmes, C. D., Tang, Q., and Prather, M. J.: Uncertainties in climate assessment for the case of aviation NO, *P. Natl. Acad. Sci. USA*, 108, 10997–11002, 2011.

5 Hoor, P., Borken-Kleefeld, J., Caro, D., Dessens, O., Endresen, O., Gauss, M., Grewe, V., Hauglustaine, D., Isaksen, I. S. A., Jöckel, P., Lelieveld, J., Myhre, G., Meijer, E., Olivier, D., Prather, M., Schnadt Poberaj, C., Shine, K. P., Staehelin, J., Tang, Q., van Aardenne, J., van Velthoven, P., and Sausen, R.: The impact of traffic emissions on atmospheric ozone and OH: results from QUANTIFY, *Atmos. Chem. Phys.*, 9, 3113–3136, doi:10.5194/acp-9-3113-2009, 2009.

10 Horowitz, L. W., Walters, S., Mauzerall, D. L., Emmons, L. K., Rasch, P. J., Granier, C., Tie, X., Lamarque, J.-F., Schultz, M. G., Tyndall, G. S., Orlando, J. J., and Brasseur, G. P.: A global simulation of tropospheric ozone and related tracers, Description and evaluation of MOZART, version 2, *J. Geophys. Res.*, 108, 4784, doi:10.1029/2002JD002853, 2003.

15 Isaksen, I. S. A., Granier, C., Myhre, G., Berntsen, T. K., Dalsøren, S. B., Gauss, M., Klimont, Z., Benestad, R., Bousquet, P., Collins, W., Cox, T., Eyring, V., Fowler, D., Fuzzi, S., Jöckel, P., Laj, P., Lohmann, U., Maione, M., Monks, P., Prevot, A. S. H., Raes, F., Richter, A., Rognerud, B., Schulz, M., Shindell, D., Stevenson, D. S., Storelvmo, T., Wang, W.-C., van Weele, M., and Wuebbles, D.: Atmospheric composition change: climate–chemistry interactions, *Atmos. Environ.*, 43, 5138–5192, 2009.

20 Johnson, C.: Impact of aircraft and surface emissions of nitrogen oxides on tropospheric ozone and global warming, *Nature*, 355, 69–71, 1992.

Johnson, C. E. and Derwent, R. G.: Relative radiative forcing consequences of global emissions of hydrocarbons, carbon monoxide and NO<sub>x</sub> from human activities estimated with a zonally-averaged two-dimensional model, *Climatic Change*, 34, 439–462, 1996.

25 Johnston, H. S.: Reduction of stratospheric ozone by nitrogen oxide catalysts from supersonic transport exhaust, *Science*, 173, 517–522, 1971.

Kinnison, D. E., Brasseur, G. P., Walters, S., Garcia, R. R., Marsh, D. A., Sassi, F., Boville, B. A., Harvey, L., Randall, C., Emmons, L., Lamarque, J.-F., Hess, P., Orlando, J., Tyndall, G., Tie, X. X., Randel, W., Pan, L., Gettelman, A., Granier, C., Diehl, T., Niemeier, U., and Simmons, A. J.: Sensitivity of chemical tracers to meteorological parameters in the MOZART-3 chemical transport model, *J. Geophys. Res.*, 112, D20302, doi:10.1029/2006JD007879, 2007.

Aviation 2006  
NO<sub>x</sub>-induced effects

A. Khodayari et al.

Title Page

Abstract

Introduction

Conclusions

References

Tables

Figures

◀

▶

◀

▶

Back

Close

Full Screen / Esc

Printer-friendly Version

Interactive Discussion



- Kinnison, D. E., Marsh, D. R., Garcia, R. R., Vitt, F., Tilmes, S., Mills, M. J., Lamarque, J.-F., Emmons, L. K., Orlando, J. J., Gettelman, A., Liu, H.-L., Yudin, V., Park, M., Randel, W., Pan, L. L., Brakebusch, M., Randall, C. E., and Hess, P.: Description and evaluation of the Whole Atmosphere Community Climate Model (WACCM): chemistry update, in preparation, 2014.
- Koffi, B., Szopa, S., Cozic, A., Hauglustaine, D., and van Velthoven, P.: Present and future impact of aircraft, road traffic and shipping emissions on global tropospheric ozone, *Atmos. Chem. Phys.*, 10, 11681–11705, doi:10.5194/acp-10-11681-2010, 2010.
- Köhler, M. O., Radel, G., Dessens, O., Shine, K. P., Rogers, H. L., Wild, O., and Pyle, J. A.: Impact of perturbations to nitrogen oxide emissions from global aviation, *J. Geophys. Res.*, 113, D11305, doi:10.1029/2007JD009140, 2008.
- Lamarque, J.-F., Emmons, L. K., Hess, P. G., Kinnison, D. E., Tilmes, S., Vitt, F., Heald, C. L., Holland, E. A., Lauritzen, P. H., Neu, J., Orlando, J. J., Rasch, P. J., and Tyndall, G. K.: CAM-chem: description and evaluation of interactive atmospheric chemistry in the Community Earth System Model, *Geosci. Model Dev.*, 5, 369–411, doi:10.5194/gmd-5-369-2012, 2012.
- Lee, D. S., Fahey, D. W., Forster, P. M., Newton, P. J., Wit, R. C. N., Lim, L. L., Owen, B., and Sausen, R.: Aviation and global climate change in the 21st century, *Atmos. Environ.*, 43, 3520–3537, 2009.
- Liang, Q., Rodriguez, J. M., Douglass, A. R., Crawford, J. H., Olson, J. R., Apel, E., Bian, H., Blake, D. R., Brune, W., Chin, M., Colarco, P. R., da Silva, A., Diskin, G. S., Duncan, B. N., Huey, L. G., Knapp, D. J., Montzka, D. D., Nielsen, J. E., Pawson, S., Riemer, D. D., Weinheimer, A. J., and Wisthaler, A.: Reactive nitrogen, ozone and ozone production in the Arctic troposphere and the impact of stratosphere-troposphere exchange, *Atmos. Chem. Phys.*, 11, 13181–13199, doi:10.5194/acp-11-13181-2011, 2011.
- Liu, X., Easter, R. C., Ghan, S. J., Zaveri, R., Rasch, P., Shi, X., Lamarque, J.-F., Gettelman, A., Morrison, H., Vitt, F., Conley, A., Park, S., Neale, R., Hannay, C., Ekman, A. M. L., Hess, P., Mahowald, N., Collins, W., Iacono, M. J., Bretherton, C. S., Flanner, M. G., and Mitchell, D.: Toward a minimal representation of aerosols in climate models: description and evaluation in the Community Atmosphere Model CAM5, *Geosci. Model Dev.*, 5, 709–739, doi:10.5194/gmd-5-709-2012, 2012.
- McElroy, M. B., Wofsy, S. C., Penner, J. E., and McConnell, J. C.: Atmospheric ozone: possible impact of stratospheric aviation, *J. Atmos. Sci.*, 31, 287–304, doi:10.1175/1520-0469(1974)031<0287:AOPIOS>2.0.CO;2, 1974.

Aviation 2006  
NO<sub>x</sub>-induced effects

A. Khodayari et al.

Title Page

Abstract

Introduction

Conclusions

References

Tables

Figures

◀

▶

◀

▶

Back

Close

Full Screen / Esc

Printer-friendly Version

Interactive Discussion



- Meinshausen, M., Raper, S. C. B., and Wigley, T. M. L.: Emulating coupled atmosphere-ocean and carbon cycle models with a simpler model, MAGICC6 – Part 1: Model description and calibration, *Atmos. Chem. Phys.*, 11, 1417–1456, doi:10.5194/acp-11-1417-2011, 2011.
- Medeiros, B., Williamson, D. L., Hannay, C., and Olson, J. G.: Southeast Pacific stratocumulus in the Community Atmosphere Model, *J. Climate*, 25, 6175–6192, 2012.
- Morrison, H. and Gettelman, A.: A new two-moment bulk stratiform cloud microphysics scheme in the NCAR Community Atmosphere Model (CAM3), Part I: Description and numerical tests, *J. Climate*, 21, 3642–3659, 2008.
- Neale, R. B., Richter, J., Park, S., Lauritzen, P. H., Vavrus, S. J., Rasch, P. J., and Zhang, M.: The mean climate of the Community Atmosphere Model (CAM4) in forced SST and fully coupled experiments, *J. Climate*, 26, 5150–5168, doi:10.1175/JCLI-D-12-00236.1, 2013.
- Neu, J. L. and Prather, M. J.: Toward a more physical representation of precipitation scavenging in global chemistry models: cloud overlap and ice physics and their impact on tropospheric ozone, *Atmos. Chem. Phys.*, 12, 3289–3310, doi:10.5194/acp-12-3289-2012, 2012.
- Olsen, S. C., Wuebbles, D. J., and Owen, B.: Comparison of global 3-D aviation emissions datasets, *Atmos. Chem. Phys.*, 13, 429–441, doi:10.5194/acp-13-429-2013, 2013a.
- Olsen, S. C., Brasseur, G. P., Wuebbles, D. J., Barrett, S., Dang, H., Eastham, S. D., Jacobson, M. Z., Khodayari, A., Selkirk, H., Sokolov, A., and Unger, N.: Comparison of model estimates of the effects of aviation emissions on atmospheric ozone and methane, *Geophys. Res. Lett.*, 40, 6004–6009, doi:10.1002/2013GL057660, 2013b.
- Patten, K. O., Khamaganov, V. G., Orkin, V. L., Baughcum, S. L., and Wuebbles, D. J.: OH reaction rate constant, IR absorption spectrum, ozone depletion potentials and global warming potentials of 2-bromo-3,3,3-trifluoropropene, *J. Geophys. Res.*, 116, D24307, doi:10.1029/2011JD016518, 2011.
- Penner, J. E., Lister, D. H., Griggs, D. J., Dokken, D. J., McFarland, M. (Eds.): Intergovernmental Panel on Climate Change, Aviation and the Global Atmosphere, Cambridge University Press, Cambridge, UK, 1999.
- Price, C., Penner, J., and Prather, M.: NO<sub>x</sub> from lightning: global distribution based on lightning physics, *Geophys. Res. Lett.*, 102, 5929–5941, 1997.
- Ridley, B., Pickering, K., and Dye, J.: Comments on the parameterization of lightning-produced NO in global chemistry-transport models, *Atmos. Environ.*, 39, 6184–6187, 2005.
- Reinecker, M. M., Suarez, M. J., Todling, R., Bacmeister, J., Takacs, L., Liu, H.-C., Gu, W., Sienkiewicz, M., Koster, R. D., Gelaro, R., Stajner, I., and Nielsen, E.: The GEOS-5 Data

Aviation 2006  
NO<sub>x</sub>-induced effects

A. Khodayari et al.

Title Page

Abstract

Introduction

Conclusions

References

Tables

Figures

◀

▶

◀

▶

Back

Close

Full Screen / Esc

Printer-friendly Version

Interactive Discussion



Assimilation System-Documentation of versions 5.0.1, 5.1.0, and 5.2.0.NASA/TM-2008-104606, Vol. 27, Technical Report Series on Global Modeling and Data Assimilation, 118 pp., available at: <http://gmao.gsfc.nasa.gov/systems/geos5/> (last access: July 2011), 2008.

Roof, C., Hansen, A., Fleming, G. G., Thrasher, T., Nguyen, A., Hall, C., Dinges, E., Bea, R., Grandi, F., Kim, B. Y., Usdrowski, S., and Hollingsworth, P.: Aviation Environmental Design Tool (AEDT) System Architecture, Doc #AEDTAD-01, USDOT Volpe Center and CSSI Inc., and ATAC Inc., and Wyle Laboratories Inc., and Georgia Tech, Cambridge, MA, 2007.

Sillman, S.: Overview: Tropospheric Ozone, Smog and Ozone-NO<sub>x</sub>-VOC Sensitivity, University of Michigan, available at: <http://www-personal.umich.edu/~sillman/Sillman-webOZONE.pdf> (last access: 11 April 2012), 2012.

Spivakovsky, C. M., Logan, J. A., Montzka, S. A., Balkanski, Y. J., Foreman-Fowler, M., Jones, D. B. A., Horowitz, L. W., Fusco, A. C., Brenninkmeijer, C. A. M., Prather, M. J., Wofsy, S. C., and McElroy, M. B.: Three-dimensional climatological distribution of tropospheric OH: update and evaluation, *J. Geophys. Res.*, 105, 8931–8980, doi:10.1029/1999JD901006, 2000.

Stevenson, D. S. and Derwent, R. G.: Does the location of aircraft nitrogen oxide emissions affect their climate impact?, *Geophys. Res. Lett.*, 36, L17810, doi:10.1029/2009GL039422, 2009.

Stevenson, D. S., Doherty, R. M., Sanderson, M. G., Collins, W. J., Johnson, C. E., and Derwent, R. G.: Radiative forcing from aircraft NO<sub>x</sub> emissions: mechanisms and seasonal dependence, *J. Geophys. Res.*, 109, D17307, doi:10.1029/2004JD004759, 2004.

Stevenson, D. S., Dentener, F. J., Schultz, M. G., Ellingsen, K., van Noije, T. P. C., Wild, O., Zeng, G., Amann, M., Atherton, C. S., Bell, N., Bergmann, D. J., Bey, I., Butler, T., Cofala, J., Collins, W. J., Derwent, R. G., Doherty, R. M., Drevet, J., Eskes, H. J., Fiore, A. M., Gauss, M., Hauglustaine, D. A., Horowitz, L. W., Isaksen, I. S. A., Krol, M. C., Lamarque, J.-F., Lawrence, M. G., Montanaro, V., Müller, J.-F., Pitari, G., Prather, M. J., Pyle, J. A., Rast, S., Rodriguez, M., Sanderson, M. G., Savage, N. H., Shindell, D. T., Strahan, S. E., Sudo, K., and Szopa, S.: Multi-model ensemble simulations of present-day and near future tropospheric ozone, *J. Geophys. Res.*, 111, D08301, doi:10.1029/2005JD006338, 2006.

Tilmes, S., Lamarque, J.-F., Emmons, L. K., Conley, A., Schultz, M. G., Saunio, M., Thouret, V., Thompson, A. M., Oltmans, S. J., Johnson, B., and Tarasick, D.: Technical Note: Ozone sonde climatology between 1995 and 2011: description, evaluation and applications, *Atmos. Chem. Phys.*, 12, 7475–7497, doi:10.5194/acp-12-7475-2012, 2012.

## Aviation 2006 NO<sub>x</sub>-induced effects

A. Khodayari et al.

Title Page

Abstract

Introduction

Conclusions

References

Tables

Figures

I◀

▶I

◀

▶

Back

Close

Full Screen / Esc

Printer-friendly Version

Interactive Discussion



Voulgarakis, A., Savage, N. H., Wild, O., Carver, G. D., Clemitshaw, K. C., and Pyle, J. A.: Upgrading photolysis in the p-TOMCAT CTM: model evaluation and assessment of the role of clouds, *Geosci. Model Dev.*, 2, 59–72, doi:10.5194/gmd-2-59-2009, 2009.

Walcek, C. J., Brost, R. A., Chang, J. S., and Wesely, M. L.: SO<sub>2</sub>, sulfate and HNO<sub>3</sub> deposition velocities computed using regional land use and meteorological data, *Atmos. Environ.*, 20, 946–964, 1986.

Walmsley, J. L. and Wesely, M. L.: Modification of coded parameterizations of surface resistances to gaseous dry deposition, *Atmos. Environ.*, 30, 1181–1188, 1996.

Wesely, M. L. and Hicks, B. B.: A review of the current status of knowledge on dry deposition, *Atmos. Environ.*, 34, 2261–2282, 2000.

Wild, O., Prather, M. J., and Akimoto, H.: Indirect long-term global cooling from NO<sub>x</sub> emissions, *Geophys. Res. Lett.*, 28, 1719–1722, 2001.

Wilkerson, J. T., Jacobson, M. Z., Malwitz, A., Balasubramanian, S., Wayson, R., Fleming, G., Naiman, A. D., and Lele, S. K.: Analysis of emission data from global commercial aviation: 2004 and 2006, *Atmos. Chem. Phys.*, 10, 6391–6408, doi:10.5194/acp-10-6391-2010, 2010.

## Aviation 2006 NO<sub>x</sub>-induced effects

A. Khodayari et al.

**Table 1.** Annual tropospheric mean burden of HO<sub>x</sub>, NO<sub>x</sub>, NO<sub>y</sub> and the ratios of OH : HO<sub>2</sub> and NO<sub>x</sub> : NO<sub>y</sub> in both CAM5 and CAM4 for both the control run (\_c) and aviation NO<sub>x</sub>-perturbed run (\_p).

	O <sub>3</sub> (kg)	OH (kg)	HO <sub>2</sub> (kg)	HO <sub>x</sub> (kg)	OH/HO <sub>2</sub>	NO <sub>x</sub> (kg N)	NO <sub>y</sub> (kg N)	NO <sub>x</sub> /NO <sub>y</sub>
CAM4_c	$3.71 \times 10^{11}$	$2.11 \times 10^5$	$2.59 \times 10^7$	$2.61 \times 10^7$	$8.15 \times 10^{-3}$	$1.20 \times 10^8$	$7.69 \times 10^8$	0.156
CAM4_p	$3.79 \times 10^{11}$	$2.17 \times 10^5$	$2.58 \times 10^7$	$2.60 \times 10^7$	$8.39 \times 10^{-3}$	$1.24 \times 10^8$	$7.96 \times 10^8$	0.156
CAM5_c	$3.26 \times 10^{11}$	$2.55 \times 10^5$	$2.75 \times 10^7$	$2.78 \times 10^7$	$9.26 \times 10^{-3}$	$1.17 \times 10^8$	$6.74 \times 10^8$	0.173
CAM5_p	$3.35 \times 10^{11}$	$2.64 \times 10^5$	$2.74 \times 10^7$	$2.77 \times 10^7$	$9.62 \times 10^{-3}$	$1.23 \times 10^8$	$7.17 \times 10^8$	0.171

Title Page

Abstract

Introduction

Conclusions

References

Tables

Figures

◀

▶

◀

▶

Back

Close

Full Screen / Esc

Printer-friendly Version

Interactive Discussion



## Aviation 2006 NO<sub>x</sub>-induced effects

A. Khodayari et al.

**Table 2.** Annual mean burden of HO<sub>x</sub>, NO<sub>x</sub>, NO<sub>y</sub> and the ratios of OH : HO<sub>2</sub> and NO<sub>x</sub> : NO<sub>y</sub> between 200–400 hPa and between 30–60° N in both CAM5 and CAM4 for both the control run (\_c) and aviation NO<sub>x</sub>-perturbed run (\_p).

	O <sub>3</sub> (kg)	OH (kg)	HO <sub>2</sub> (kg)	HO <sub>x</sub> (kg)	OH/HO <sub>2</sub>	NO <sub>x</sub> (kg N)	NO <sub>y</sub> (kg N)	NO <sub>x</sub> /NO <sub>y</sub>
CAM4_c	$2.77 \times 10^{10}$	$9.61 \times 10^3$	$7.95 \times 10^5$	$8.04 \times 10^5$	$1.21 \times 10^{-2}$	$4.54 \times 10^6$	$4.48 \times 10^7$	0.10
CAM4_p	$2.89 \times 10^{10}$	$1.09 \times 10^4$	$7.57 \times 10^5$	$7.67 \times 10^5$	$1.44 \times 10^{-2}$	$6.39 \times 10^6$	$5.28 \times 10^7$	0.12
CAM5_c	$2.64 \times 10^{10}$	$1.30 \times 10^4$	$8.79 \times 10^5$	$8.92 \times 10^5$	$1.47 \times 10^{-2}$	$4.80 \times 10^6$	$4.85 \times 10^7$	0.10
CAM5_p	$2.78 \times 10^{10}$	$1.47 \times 10^4$	$8.25 \times 10^5$	$8.40 \times 10^5$	$1.78 \times 10^{-2}$	$7.03 \times 10^6$	$6.13 \times 10^7$	0.11

Title Page

Abstract

Introduction

Conclusions

References

Tables

Figures

◀

▶

◀

▶

Back

Close

Full Screen / Esc

Printer-friendly Version

Interactive Discussion





Aviation 2006  
NO<sub>x</sub>-induced effects

A. Khodayari et al.

Title Page

Abstract

Introduction

Conclusions

References

Tables

Figures

I◀

▶I

◀

▶

Back

Close

Full Screen / Esc

Printer-friendly Version

Interactive Discussion



**Table 3.** Global annual average CH<sub>4</sub> lifetimes against reaction with OH, as calculated by CAM4 and CAM5 for the control run and for the NO<sub>x</sub> perturbation run. The relative change between runs is displayed in the right-most column. It is noted that the calculated lifetimes are shorter than the CH<sub>4</sub> lifetime derived based on Methyl chloroform analysis (Prather et al., 2012).

CH <sub>4</sub> lifetime (yr)	Control run	Perturbed run	Rel change (%)
CAM5	7.35	7.21	1.90
CAM4	8.83	8.71	1.40

# Aviation 2006 NO<sub>x</sub>-induced effects

A. Khodayari et al.

Title Page

Abstract

Introduction

Conclusions

References

Tables

Figures

◀

▶

◀

▶

Back

Close

Full Screen / Esc

Printer-friendly Version

Interactive Discussion

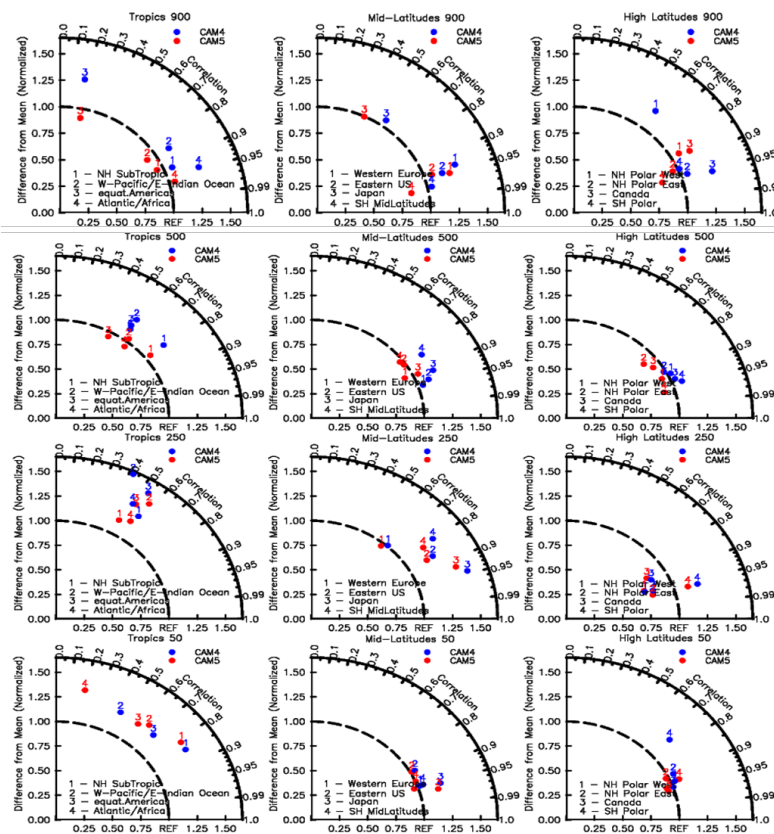


**Fig. 1.** Taylor diagram of modelled ozone against ozonesonde climatology for four pressure levels and three latitudinal regions. REF along the abscissa denotes the observations while the radial distance describes the normalized bias. The correlation for the seasonal cycle is described along the angle.

Aviation 2006  
NO<sub>x</sub>-induced effects

A. Khodayari et al.

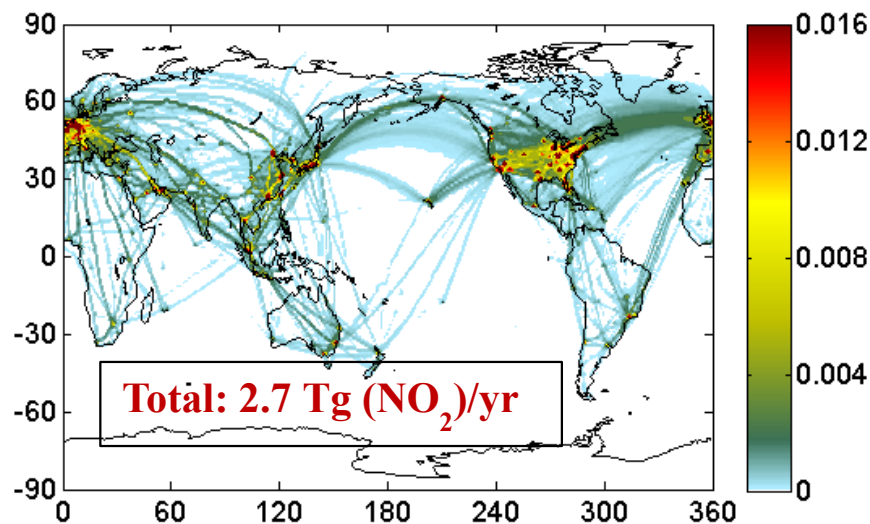


**Fig. 2.** Spatial distribution of vertically-integrated aviation NO<sub>x</sub> emissions for 2006.

Title Page

Abstract

Introduction

Conclusions

References

Tables

Figures

◀

▶

◀

▶

Back

Close

Full Screen / Esc

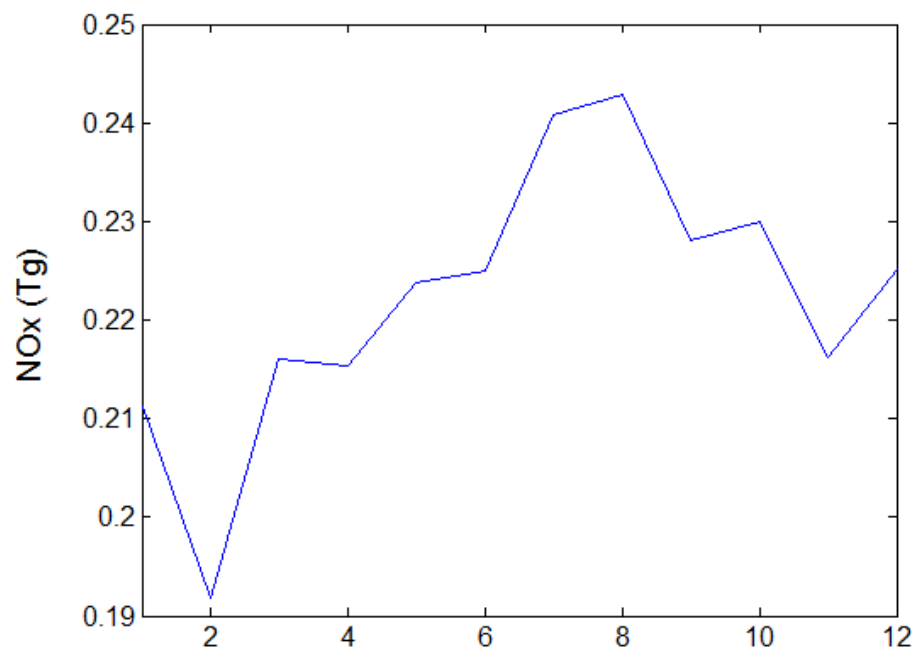
Printer-friendly Version

Interactive Discussion



**Aviation 2006  
NO<sub>x</sub>-induced effects**

A. Khodayari et al.

**Fig. 3.** Seasonal distribution of global aviation NO<sub>x</sub> emissions for 2006.

Title Page

Abstract

Introduction

Conclusions

References

Tables

Figures

I◀

▶I

◀

▶

Back

Close

Full Screen / Esc

Printer-friendly Version

Interactive Discussion



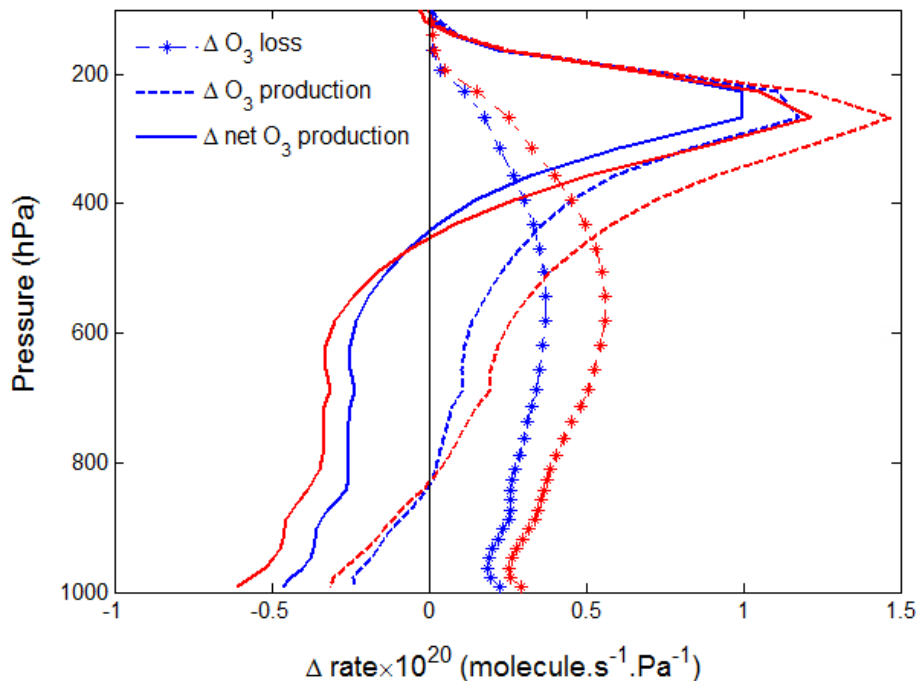


**Fig. 4.** Vertical profile describing the aviation  $\text{NO}_x$ -induced change in the rate of  $\text{O}_3$  production with height (results are shown in red for CAM5 and in blue for CAM4). Net rate of ozone production (solid line), the gross rate of ozone production (dashed line), and the rate of ozone loss (dotted line) are shown. Production and loss rates are calculated as zonal and meridional means.

Aviation 2006  
NO<sub>x</sub>-induced effects

A. Khodayari et al.

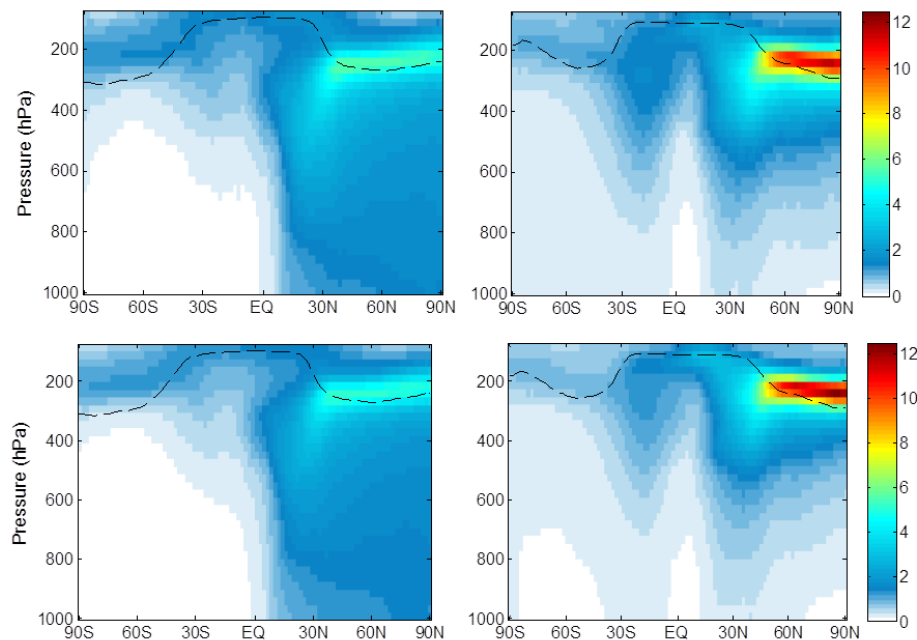


**Fig. 5.** Zonal mean perturbations of ozone (ppb) during January (left) and July (right). CAM5 is in the top panel, while CAM4 is on the bottom. The dashed line indicates the tropopause.

Title Page

Abstract

Introduction

Conclusions

References

Tables

Figures

I◀

▶I

◀

▶

Back

Close

Full Screen / Esc

Printer-friendly Version

Interactive Discussion



Aviation 2006  
NO<sub>x</sub>-induced effects

A. Khodayari et al.

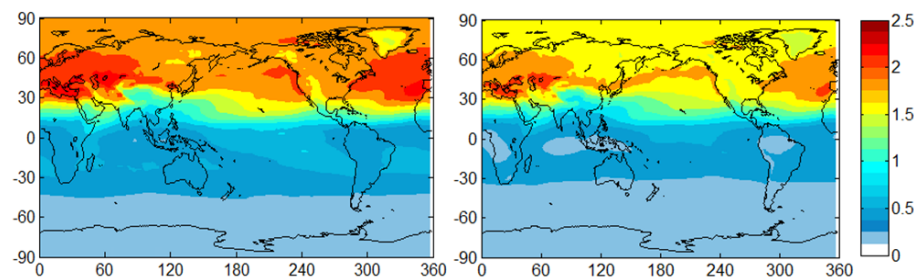


**Fig. 6.** Yearly mean perturbations of the ozone column ( $\Delta\text{DU}$ ) based on 2006 aircraft NO<sub>x</sub> emissions. CAM5 is on the left, while CAM4 is on the right.

Title Page

Abstract

Introduction

Conclusions

References

Tables

Figures

I◀

▶I

◀

▶

Back

Close

Full Screen / Esc

Printer-friendly Version

Interactive Discussion





Aviation 2006  
NO<sub>x</sub>-induced effects

A. Khodayari et al.

Title Page

Abstract

Introduction

Conclusions

References

Tables

Figures

◀

▶

◀

▶

Back

Close

Full Screen / Esc

Printer-friendly Version

Interactive Discussion

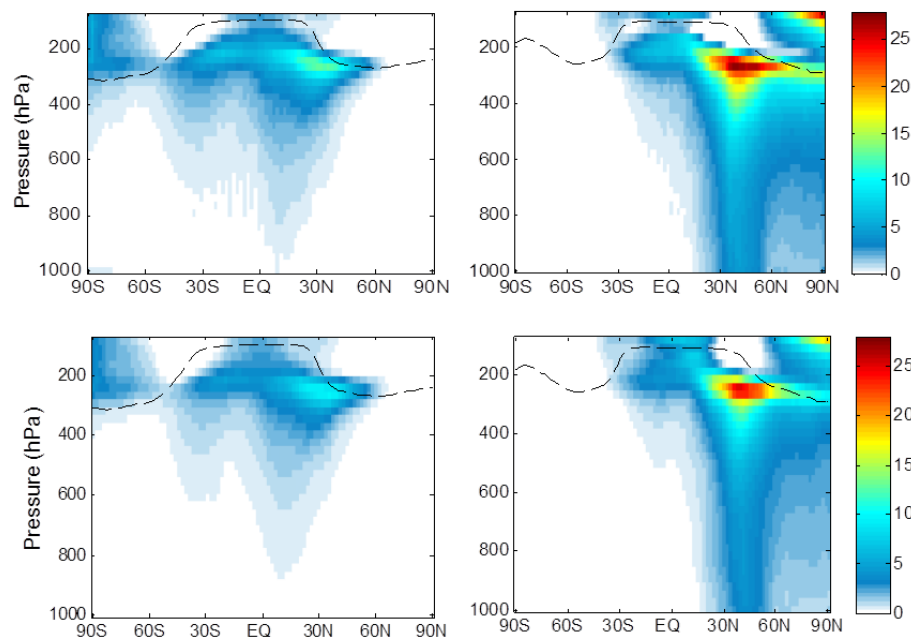


**Fig. 7.** Aviation induced OH perturbations ( $10^{-4} \Delta$  molecules  $\text{cm}^{-3}$ ) during January (left) and July (right). CAM5 is in the top panel, while CAM4 is in the bottom. The dashed line indicates the tropopause.

Aviation 2006  
NO<sub>x</sub>-induced effects

A. Khodayari et al.

Title Page

Abstract

Introduction

Conclusions

References

Tables

Figures

I◀

▶I

◀

▶

Back

Close

Full Screen / Esc

Printer-friendly Version

Interactive Discussion

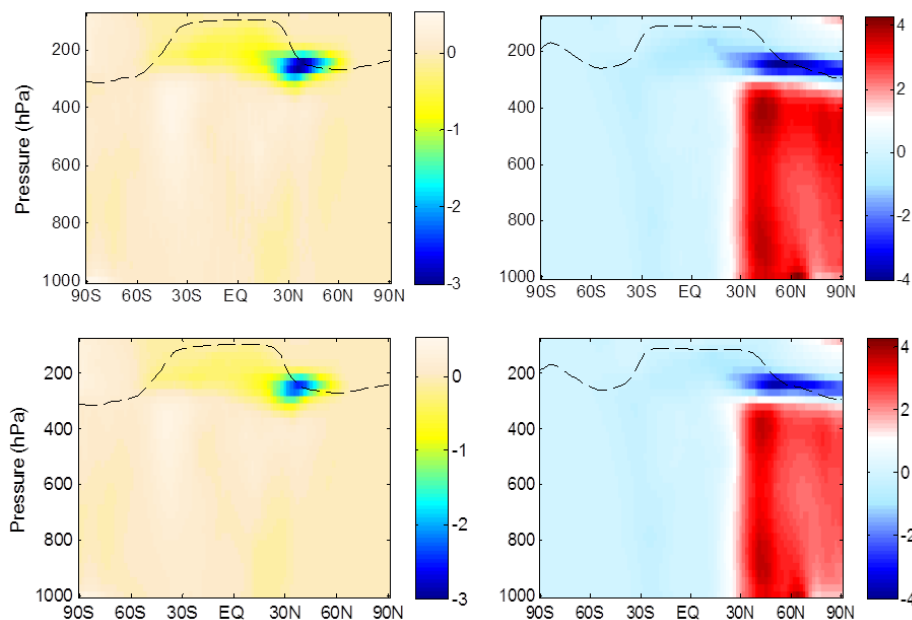


**Fig. 8.** As in Fig. 7, but for HO<sub>2</sub> ( $10^{-6} \Delta$  molecules cm<sup>-3</sup>).

Aviation 2006  
NO<sub>x</sub>-induced effects

A. Khodayari et al.

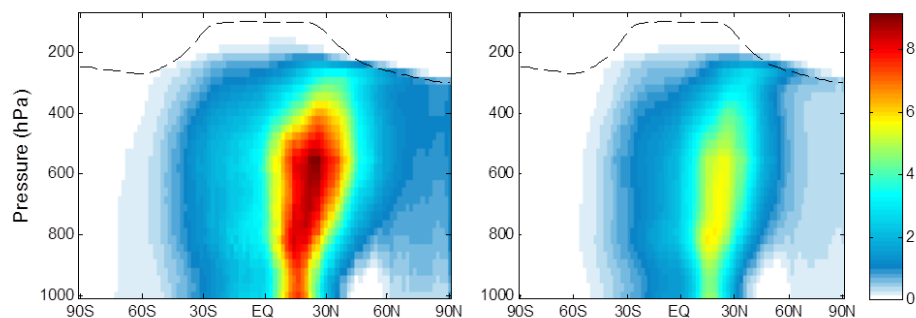


**Fig. 9.** Annual zonal averaged CH<sub>4</sub> loss ( $10^{-3} \Delta \text{molecules cm}^{-3} \text{s}$ ) induced by aviation NO<sub>x</sub> emissions. CAM5 is on the left, CAM4 is on the right. The dashed line indicates the tropopause.

Title Page

Abstract

Introduction

Conclusions

References

Tables

Figures

I◀

▶I

◀

▶

Back

Close

Full Screen / Esc

Printer-friendly Version

Interactive Discussion



Aviation 2006  
NO<sub>x</sub>-induced effects

A. Khodayari et al.

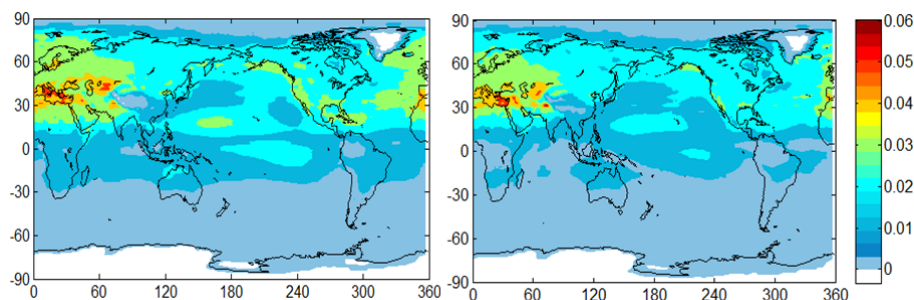


**Fig. 10.** Yearly mean radiative forcing ( $\text{mW m}^{-2}$ ) from  $\text{O}_3$  due to aviation  $\text{NO}_x$  emissions. CAM5 is on the left, CAM4 is on the right.

Title Page

Abstract

Introduction

Conclusions

References

Tables

Figures

I◀

▶I

◀

▶

Back

Close

Full Screen / Esc

Printer-friendly Version

Interactive Discussion

